# Reducing Radicals in Nitrate Solutions. The $NO_3^{2-}$ System Revisited

**Andrew R. Cook,[†] Nada Dimitrijevic,[‡] Benjamin W. Dreyfus,[§] Dan Meisel,*[,§] Larry A. Curtiss,[‡] and Donald M. Camaioni*[,||]**

*Chemistry Department, Brookhaven National Laboratory, Upton, New York 11973, Chemistry Division, Argonne National Laboratory, Argonne, Illinois 60439, The Radiation Laboratory and the Department of Chemistry and Biochemistry, University of Notre Dame, Notre Dame, Indiana 46556, and Environmental Molecular Sciences Laboratory, Pacific Northwest National Laboratory, Richland, Washington 99352*

*Received: October 16, 2000; In Final Form: February 7, 2001*

The one-electron reduction product of nitrate, the $NO_3^{2-}$ radical, was reinvestigated because of the contemporary interest in its reactivity in high-level liquid radioactive systems. Indirect observations suggest that the same dianion is produced by the precursor to the solvated electron. The redox potential of the couple $NO_3^-/NO_3^{2-}$ was calculated, using several ab initio approaches combined with semiempirical solvation models, to be $E^\circ \approx -1.1$ V vs NHE. Using the theoretical prediction to guide the experiment, we find a value of $E^\circ = -0.89$ V at zero ionic strength. Kinetic and free-energy-relationship arguments are used to question the acid−base equilibria and reaction mode that converts the $NO_3^{2-}$ to the oxidizing $NO_2$ radical. It is proposed that the reaction of the dianion with various general acids is an $O^{2-}$ (i.e., water or $OH^-$) transfer to the acid and not proton transfer to $NO_3^{2-}$. Implications of the highly negative redox potential of the dianion and the existence of the protonated forms to practical systems are discussed.

## Introduction

The oxidizing radicals from nitrate and nitrite, the $NO_x$ ($x = 1-3$) family, received much attention in the past decade because of their adverse effects in atmospheric processes and because of their participation in various biochemical−physiological reactions. The reducing radicals obtained from reduction of their parent ions, $NO_x^{2-}$, were less studied. Our current interest in both classes of radicals stems from the dominant role that they play in irradiated aqueous solutions of nitrate and nitrite, in particular, as they relate to radioactive waste forms. Much of the high level nuclear waste, temporarily stored in large tanks in the U.S., is in concentrated solutions of $NO_3^-$ and $NO_2^-$; therefore, the radiation chemistry of these solutions has many practical implications to nuclear waste management. In this study we revisit the reducing radicals that are generated from nitrate.

Much of the information on the chemistry that is initiated by the absorption of ionizing radiation in nitrate solutions is due to the early work of Gratzel et al.[1] The reaction of solvated electron with nitrate produces the dianion radical $NO_3^{2-}$, which in turn reacts with water to generate the $NO_2$ radical (reaction 1 and 2).[2]

$$e^-_{aq} + NO_3^- \rightarrow NO_3^{2-} \qquad k_1 = 9.7 \times 10^9\ M^{-1}\ s^{-1} \quad (1)$$

$$NO_3^{2-} + (H_2O) \rightarrow NO_2 + 2OH^- \qquad k_2 = 5.5 \times 10^4\ s^{-1} \quad (2)$$

Thus, the strongly reducing $NO_3^{2-}$ radical can persist in solution for no more than ~20 $\mu$s before it is converted into the oxidizing $NO_2$ radical [$E^\circ_{(NO_2/NO_2^-)} = 1.04$ V[3]]. The same oxidizing radical is produced by the reaction of hydroxyl radical with nitrite in the radiolysis of aqueous $NO_2^-$ solutions. Hydrogen atoms that are generated by the radiolysis of water are converted in the high-level liquid waste solutions to NO radicals via their reaction with nitrite [$E^\circ_{(NO/NO^-)} = -0.35$ and 0.39 V for the singlet and triplet, respectively[3]]. The practical implication of this scheme of reactions is that $NO_3^{2-}$ is the major radical that can produce fuels in radioactive solutions but only in the time window of ~1 ps to ~20 $\mu$s after the absorption of radiation by the solution. At shorter times, electrons (hydrated or their precursor) are still available and at longer times the solution contains only oxidizing radicals.

Reactions 3 and 4 describe the acid−base equilibria of the one-electron reduced nitrate as reported in the literature.[1]

$$HNO_3^- \rightleftarrows H^+ + NO_3^{2-} \qquad pK_{a1} = 7.5 \quad (3)$$

$$H_2NO_3 \rightleftarrows H^+ + HNO_3^- \qquad pK_{a2} = 4.8 \quad (4)$$

Furthermore, these reports indicate that the lifetimes of the three forms of the radical decrease progressively upon protonation:[1,4]

$$HNO_3^- \rightarrow NO_2 + OH^- \qquad k_5 = 2.3 \times 10^5\ s^{-1} \quad (5)$$

$$H_2NO_3 \rightarrow H_2O + NO_2 \qquad k_6 = 7.0 \times 10^5\ s^{-1} \quad (6)$$

The early reports also noted that the lifetime of the dianion

* To whom correspondence should be addressed. (D.M.) Fax: (219) 631-3646. E-mail: dani@nd.edu. (D.M.C.) Fax: (509) 375-6660. E-mail: donald.camaioni@pnl.gov.
[†] Chemistry Department.
[‡] Chemistry Division.
[§] The Radiation Laboratory and the Department of Chemistry and Biochemistry.
[||] Environmental Molecular Sciences laboratory.

10.1021/jp0038052 CCC: $20.00 
Published on Web 03/16/2001

decreases when other proton donors, specifically $H_2PO_4^-$, were added to the solution.[1]

$$NO_3^{2-} + H_2PO_4^- \rightleftarrows HNO_3^- + HPO_4^{2-} \qquad k_7 = 5.0 \times 10^8\ M^{-1}\ s^{-1} \quad (7)$$

This led to the recognition that general acids can exchange protons with $NO_3^{2-}$ radicals (reaction 8) and later reports extended these observations to other proton donors, such as ammonium ions:[5,4]

$$NO_3^{2-} + HA \rightleftarrows HNO_3^- + A^- \quad (8)$$

The reports on the reaction of general acids with the radical dianion drew our attention to this system. Acids with p$K_a$s that are 2 units higher than that of $NO_3^{2-}$ should not noticeably reduce its lifetime if equilibrium 8 is established. We verify in the present study that many general Lewis acids react with $NO_3^{2-}$, but we conclude that this reaction cannot be represented by proton-transfer equilibrium of reaction 8. This leads us to question the existence of the protonated species. Indeed, it is unusual for successive dissociation constants of oxy acids (reactions 3 and 4) to differ by less than 4 p$K_a$ units.[40] We suggest that $O^{2-}$ is transferred to the acid to produce directly $NO_2$. To assist in the understanding of the properties of $NO_3^{2-}$ radical, we calculated its redox potential and studied the role of $HNO_3^-$ using a combination of ab initio and semiempirical computational methods. The calculated redox potential then guides us in the selection of appropriate reference redox couples that are used to experimentally determine the redox potential of the $NO_3^-/NO_3^{2-}$ couple. We also show that the product of the reaction of the presolvated electron with nitrate is a strongly reducing radical, presumably the same radical dianion.

## Experimental Section

*Chemicals.* All chemicals used were of the highest quality commercially available; Nanopure water from a Barnstead ultrapure water system was used throughout. Stock solutions were prepared fresh prior to irradiation. All solutions were degassed by bubbling ultrapure argon, or saturated with $N_2O$, prior to irradiation. The bridged bipyridinium salt 2,2′-tetramethylene bipyridinium (labeled $V^{2+}$) dibromide was synthesized following literature procedures,[6] and its redox potential was taken to be −0.650 V vs NHE.[7] Elemental analysis indicated that it crystallized with a molecule of hydrogen bromide per every five $VBr_2$ molecules similar to previous observations.[6] The slight excess of bromide had no implication on the radiolytic results and no indication of generation of $Br_2^-$ radicals could be observed in any of the experiments where this salt was used.

*Radiolysis Experiments.* Electron pulses of 4−40 ns width, from the Argonne electron linear accelerator were used to produce $0.5 \times 10^{-6}$ to $2.2 \times 10^{-5}$ M hydrated electrons. Measurements were made using 1, 2, or 4 cm Suprasil cells but all the results presented here were normalized to 1-cm optical path. A pulsed xenon lamp was used as the analyzing light source. An $N_2O$ saturated aqueous solution of 10 mM KSCN was used for dosimetry and the extinction coefficient of $(SCN)_2^-$ at $\lambda = 478$ nm was assumed to be 7600 $M^{-1}\ cm^{-1}$. Dosimetry for conductivity experiments was done using saturated $CH_3Cl$ solutions at pH 4 assuming $\lambda(H^+) = 350$ S cm$^2$ mole$^{-1}$, $\lambda(OH^-) = 199$ S cm$^2$ mol$^{-1}$, and $\lambda(Cl^-) = 76$ S cm$^2$ mol$^{-1}$. Details of the conductivity apparatus and its calibration have been previously described.[8] Unless otherwise stated, solutions contained $10^{-2}$ M of *tert*-butyl alcohol to scavenge OH radicals.

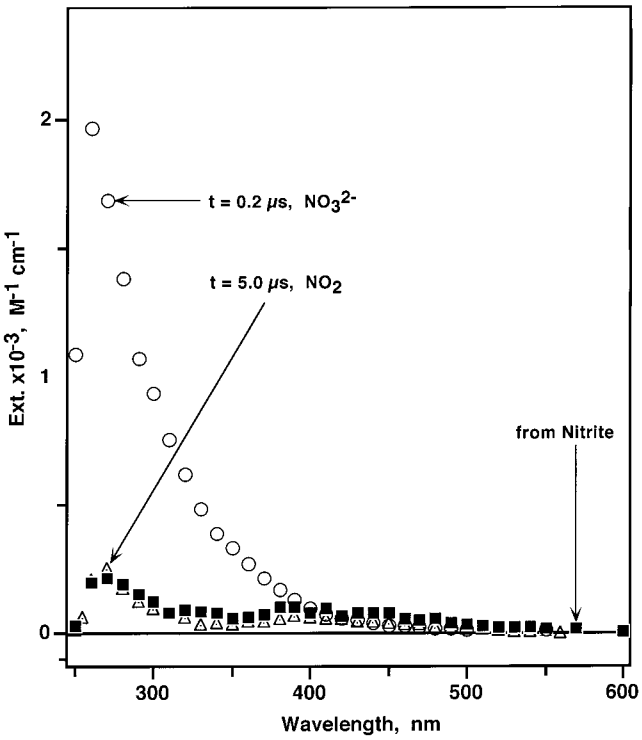


**Figure 1.** Spectra of the radicals obtained upon irradiation of nitrate and nitrite solutions. Open data points: 20 mM $NaNO_3$ at pH 10.2 with 40 mM CAPS buffer. Circles are 0.2 $\mu$s and triangles are 5 $\mu$s after the pulse. Solid squares are from $N_2O$ saturated solution containing 20 mM $NaNO_2$.

*Theoretical Methods.* The geometries of species relevant to reactions involving $NO_3^{2-}$ were determined at the HF/6-31G* and MP2(full)/6-31G* levels of theory.[9] The energies of the gas-phase species were calculated using Gaussian-2 (G2) theory,[10] a theoretical method capable of calculating gas-phase reaction energies accurate to ±2 kcal/mol.[11] All of the gas-phase calculations were performed using the GAUSSIAN-94 computer program.[12] Solvent effects were included in self-consistent field (SCF) calculations using either Tomasi's polarized continuum model (PCM)[13] with GAUSSIAN-94 or the SM1 and SM2.2 (SMx) models developed by Cramer and Truhlar with the AMSOL program.[14,15] The solvation enthalpy using the PCM method is determined in an ab initio HF/6-31G* calculation where the solvent is modeled as a polarizable continuum of a uniform dielectric constant, with a form-fitting cavity for the molecule of interest. In contrast, the SM1 and SM2.2 methods determine the solvation free energy in aqueous solution using the AM1 Hamiltonian,[14,15] where the solvent is modeled not only as a form-fitting polarizable dielectric, but which also explicitly includes terms describing cavitation, dispersion, solvent structure, and hydrophobic effects using an empirical function.

## Results and Discussion

*Identification of Intermediates.* Figure 1 shows the spectrum of the product obtained at the end of reaction 1 following pulse irradiation of a $2 \times 10^{-2}$ M $NaNO_3$ deaerated solution containing $4 \times 10^{-2}$ M CAPS (3-cyclohexylamino-1-propanesulfonic acid) buffer at pH 10.2. This spectrum is similar to that reported earlier for $NO_3^{2-}$; we obtain $\epsilon = 2.0 \times 10^3\ M^{-1}\ cm^{-1}$ at $\lambda_{max} = 260$ nm. It decays within a few microseconds to generate the weak spectrum shown in Figure 1 at 5 $\mu$s after the pulse. The broad band at $\lambda_{max} = 390$ nm in the 5 $\mu$s spectrum is similar to the one reported for $NO_2$.[16] The additional band at

$\lambda_{max} = 270$ nm probably results from a small fraction of the $NO_2$ that has already dimerized to $N_2O_4$.[16]

$$2NO_2 \rightleftarrows N_2O_4 \qquad 2k_9 = 9.0 \times 10^8\ M^{-1}\ s^{-1} \qquad (9)$$

$$k_{-9} = 6.9 \times 10^3\ s^{-1}$$

For comparison, Figure 1 also includes a spectrum obtained from irradiation of an $N_2O$ saturated solution containing $5 \times 10^{-2}$ M $NaNO_2$. This spectrum is believed to represent generation of authentic $NO_2$ via the sequence of reactions 10 and 11:[2,4]

$$e^-_{aq} + N_2O \xrightarrow{H_2O} OH + N_2 + OH^- \qquad k_{10} = 9.1 \times 10^9\ M^{-1}\ s^{-1} \qquad (10)$$

$$NO_2^- + OH \rightarrow NO_2 + OH^- \qquad k_{11} = 6.0 \times 10^9\ M^{-1}\ s^{-1} \qquad (11)$$

It is concluded that the two weak spectra are identical. Similar spectra were obtained using phosphate (pH 7.1) and borate (pH 9.2) buffers and in acidic solution (pH 4.5), indicating that the same product is eventually produced in all of these experiments.

The charge of the initial product was verified to be $-2$ by measuring the ionic strength effect on the rate of electron transfer from the radical anion to methyl viologen ($MV^{2+}$) according to reaction 12. The rate constant for that reaction was previously determined to be $3.3 \times 10^9\ M^{-1}\ s^{-1}$.[17]

$$NO_3^{2-} + MV^{2+} \rightarrow NO_3^- + MV^+ \qquad (12)$$

As can be expected from the charge of the reactants, the rate should be sensitive to the ionic strength of the solution. Figure 2 shows the rate constant as a function of $\mu$, the ionic strength, which was controlled by varying the concentration of $NaNO_3$. The rate was measured at $\lambda = 600$ and 394 nm, the strong bands of the $MV^+$ product. A least-squares fit to the Brönsted-Bjerrum modified Debye−Huckel equation, eq 13,

$$\log\frac{k}{k_0} = \frac{1.018 Z_a Z_b \sqrt{\mu}}{1 + 0.329 d \sqrt{\mu}} \qquad (13)$$

yields: the rate constant at zero ionic strength, $k_0 = (1.3 \pm 0.1) \times 10^{10}\ M^{-1}\ s^{-1}$, the product of the charges, $Z_aZ_b = -4.2 \pm 0.2$, and an effective reaction distance $d = 2.48 \pm 0.2$ Å. Both the absorption spectrum and the product of charges lead us to conclude that the initial intermediate discussed here is indeed $NO_3^{2-}$ and its product is eventually $NO_2$.

*Reactions of the Precursor of Hydrated Electrons*. The experiments described in Figure 2 provide an opportunity to probe the products of the reaction of the precursor to the hydrated electron with nitrate (reaction 1a). We label that precursor as $e^-_{th}$ without committing to its

$$e^-_{th} + NO_3^- \rightarrow P \qquad (1a)$$

exact identity except to indicate that it is thermalized. The nitrate ion is one of the most efficient scavengers for that precursor; the concentration at which only 37% of the initially produced thermal electrons escape scavenging, is $C_{37} = 0.45$ M.[18,19] Because of the low $C_{37}$ and because the concentration of nitrate in many practical situations is extremely high (1−5 M), the identity of the product, *P* in reaction 1a, is of considerable

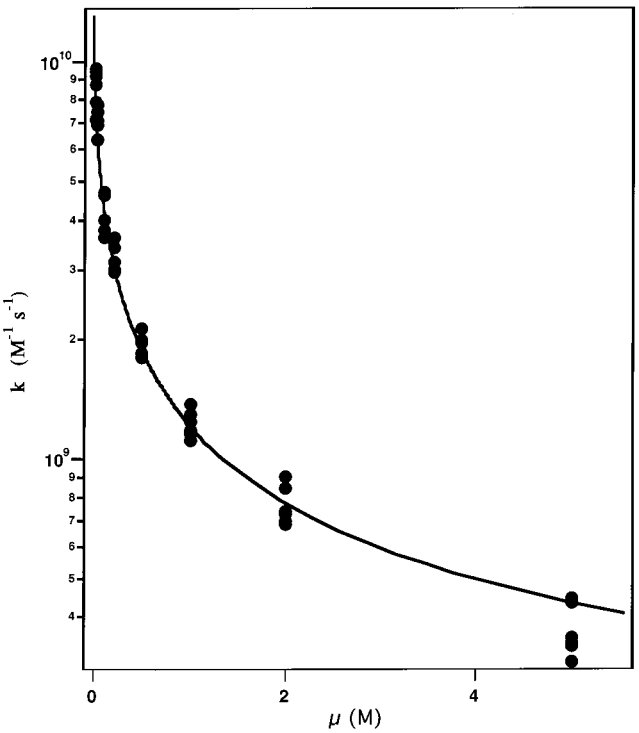


**Figure 2.** Dependence of the rate constant for the reaction of $NO_3^{2-}$ with methyl-viologen ($MV^{2+}$) on ionic strength. The rate was measured at the $MV^+$ bands at $\lambda = 600$ and 394 nm. Ionic strength was varied by changing [$NaNO_3$]. Solid curve is the least-squares fit to eq 13 using $k_0 = 1.3 \times 10^{10}\ M^{-1}\ s^{-1}$, $Z_aZ_b = -4.2$ and $d = 2.48$ Å.

significance. To test that question, we measured the yield of $MV^+$ from reaction 12 at increasing $NaNO_3$ concentrations. The normalized absorbance from $MV^+$, as determined at 600 and 394 nm, at several doses in the range of 0.25−0.50 krad/pulse, is given in Figure 3. We chose to use low doses because the rate of formation of $MV^+$ becomes slow at high ionic strength and therefore recombination of radicals becomes significant under such conditions.

As can be seen in Figure 3, up to 30% decrease in the yield of $MV^+$ can be observed at 5 M of $NaNO_3$. Several factors, real or artifacts, were considered as probable causes for the observed decrease. The high ionic strength may modify the spectrum of $MV^+$. However, the spectrum at low and high nitrate concentrations revealed no spectral differences (except at <300 nm where $NO_2$, and other $NO_x$ products from direct effects, absorb light). Ion-pairing of the parent molecules, or the radicals, as a cause for the reduced yield was also rejected because the zwitterionic viologen 4,4′-bis(propyl-sulfonato) bipyridinium (ZV) gave the same results, within experimental error, as $MV^{2+}$. On the other hand, some of the radiation is absorbed directly by the nitrate salt. Assuming that this "direct effect" is proportional to the electron density of each component, 37% of the radiation is directly absorbed by nitrate at 5 M concentration. That fraction, similar to the reduction in the yield of viologen radicals, produces directly $NO_2$, and perhaps NO, but not the reducing $NO_3^{2-}$.[20−24] Thus, we conclude that the reaction of the precursor to the hydrated electron with nitrate produces a reducing radical, presumably the same $NO_3^{2-}$ radical dianion.

*Acid−Base Reactions of the Intermediates*. Unless otherwise specified, the rate of the decay of $NO_3^{2-}$ in all experiments described below was measured at $\lambda = 270$ nm. Figure 4 describes the dependence of the rate of $NO_3^{2-}$ decay on

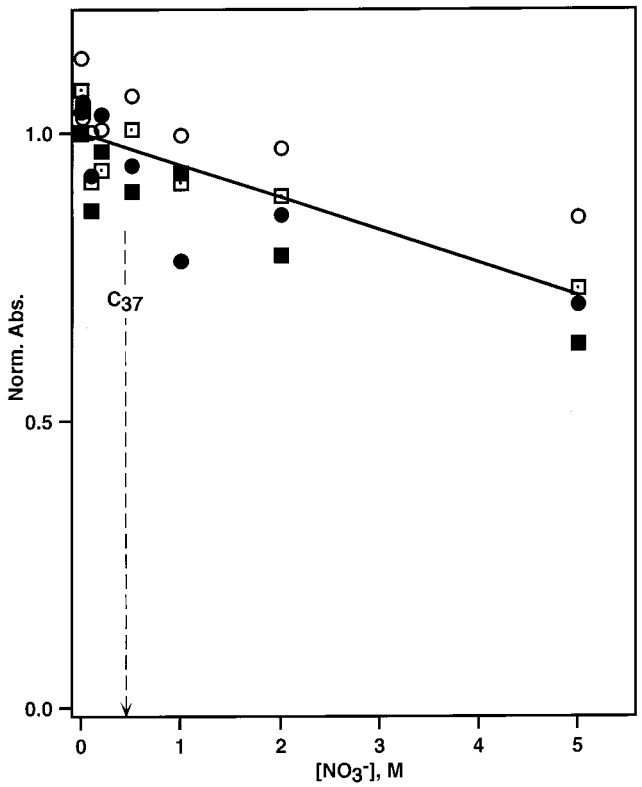


**Figure 3.** Dependence of the yield of methyl-viologen radicals ($MV^+$), normalized to the yield at low ionic strength, on nitrate concentration. Absorbance was measured at the $MV^+$ bands at $\lambda = 600$ and 394 nm. Doses in the pulse range from 0.25 to 0.50 krad/pulse. All solutions contained 1 mM $MV^{2+}$. The vertical arrow indicates the concentration at which the yield of $e^-_{aq}$ is reduced to $1/e$ (37%) of the yield at low nitrate concentration.

concentration of boric acid, $B(OH)_3$, at constant total borate concentration. It is clear from that figure that the acid form of the borate buffer reacts much faster than the basic form. This is a general observation for all buffer systems studied here. Table 1 compiles the rate constants for the reaction of various "acids" with $NO_3^{2-}$. All were obtained from the dependence of the rate of decay of the radical dianion on the concentration of the acid form of the buffer. All rates were measured at various doses in the range described in the Experimental Section and extrapolated to zero dose as in the inset to Figure 4. This corrects for the small dose effects that result from the contribution of radical−radical reactions.

As can be seen in Table 1, those rate constants that were determined previously are in reasonable agreement with the present results. However, several cases in Table 1 require a comment. In the case of $H^+$, measurements were made in the pH range of 4−5. The concentration of $H^+$ was corrected for the production of protons by the radiolysis. We assume the yield $G(H^+) = G(e^-_{aq})$ for this correction (all yields are expressed as $G$-value in molecules per 100 eV). As the rate constants in Table 1 decrease, the accuracy of the measurement also decreases. At the highest concentration of methanol used (5 M), the rate is only 50% faster than at very low methanol concentration. Thus, the large error limits for the smaller rate constants.

Results from experiments to measure the rate constant of reaction 8 with the acidic and basic form of ammonia are shown in Figure 5. The rate with $NH_4^+$ was measured at constant pH 9.1 and at relatively low total ammonia concentrations. Assuming (as in the case of borate) that the rate of reaction with $NH_3$ is much slower than with $NH_4^+$, the rate constant extracted then

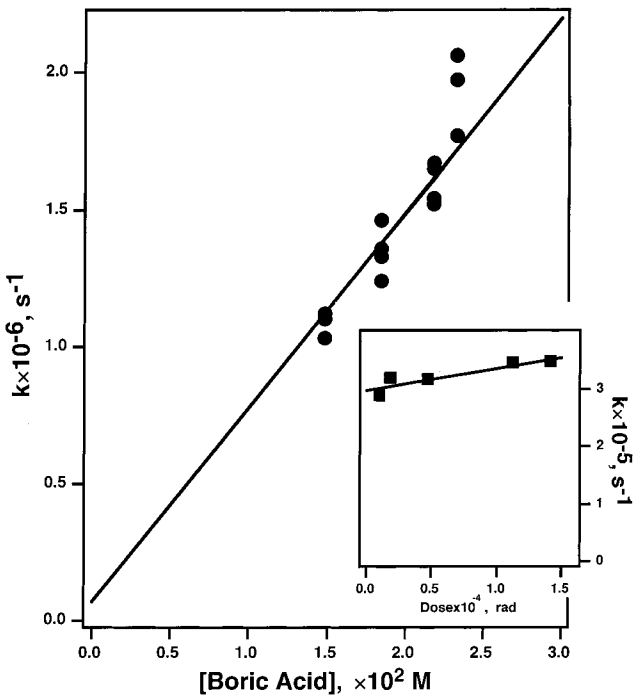


**Figure 4.** Dependence of the pseudo first-order rate constant for disappearance of $NO_3^{2-}$, measured at 270 nm, on concentration of boric acid. All solutions contained $[NaNO_3] = 2.5 \times 10^{-2}$ M and constant $[Borate]_{tot} = 2.5 \times 10^{-2}$ M, pH varied in the range 5.7−8.1. (Inset) Dependence of the rate on dose, measured at $[B(OH)_3] = 2.5 \times 10^{-3}$ M. Rates are extrapolated to zero dose as shown in the inset.

**TABLE 1: Rate Constants for the Reaction of Various "Acids" with $NO_3^{2-}$**

| HA | $k$ ($M^{-1}\,s^{-1}$) | p$K_a$ | Lit. $k$ ($M^{-1}\,s^{-1}$) | ref |
|---|---|---|---|---|
| $H^+$ | $(4.5 \pm 0.5) \times 10^{10}$ | | $\gg 2.0 \times 10^{10}$ [a] | *5* |
| $H_2PO_4^-$ | $(5.3 \pm 0.5) \times 10^8$ | 7.21 | $5.0 \times 10^8$ | *1* |
| $NH_4^+$ | $(3.6 \pm 0.4) \times 10^8$ | 9.25 | $2.0 \times 10^8$ | *5* |
| $B(OH)_3$ | $(8.4 \pm 0.8) \times 10^7$ | 9.24 | | |
| $HCO_3^-$ | $2.8 \times 10^7$ | 10.3 | | *37* |
| $CAPSH^+$ | $(1.1 \pm 0.1) \times 10^7$ | 10.4 | | |
| $NH_3$ | $(3.4 \pm 0.6) \times 10^6$ | | | |
| MeOH | $(1.2 \pm 0.4) \times 10^4$ | 15.0 | | |
| *t*-BuOH | $\leq 2 \times 10^4$ | 16.9 | | |
| $H_2O$ | $(1.2 \pm 0.1) \times 10^3$ | 15.7 | $1.00 \times 10^3$ | *1* |
| | $(6.8 \pm 0.8 \times 10^4\,s^{-1})$ | | | *4* |

[a] An unreasonably small value of $5.0 \times 10^8$ $M^{-1}$ $s^{-1}$ is given in ref *35*.

is for the reaction with the ammonium ion (Figure 5, circles). The rate was then measured at varying $NH_3/NH_4^+$ ratios and the contribution from the reaction with the $NH_4^+$ ion was subtracted from the observed rate. The results (Figure 5, squares) yield a rate constant with $NH_3$ that is smaller than that with the ion by a factor of ~100. $NH_3$ is not a common proton donor, and it is not easy to visualize a mechanism by which it protonates the $NO_3^{2-}$ radical. Reaction 14, proton transfer from hydrated ammonia, concerted with N−O scission-in effect, an oxide ion, $O^{2-}$, transfer from $NO_3^{2-}$ concerted with protonation-is a plausible mechanism.

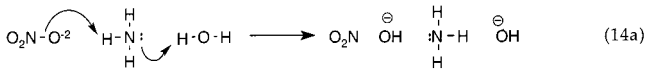


(14a)

The reverse reaction, addition of $O^{2-}$ to $NO_2$ radicals, was recently explored but only vestiges of such a possible reaction observed.[38]

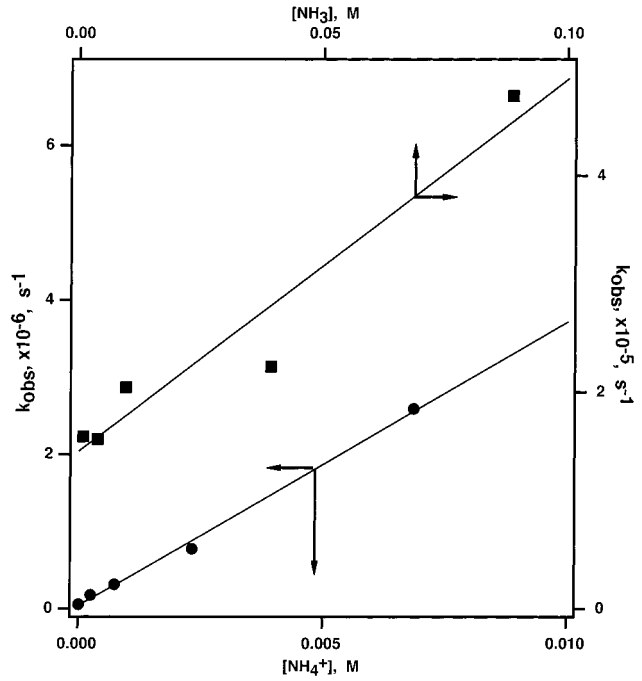


**Figure 5.** Dependence of the pseudo-first-order rate constant for disappearance of $NO_3^{2-}$ on concentration of ammonium ions (circles; bottom and left axes) and ammonia (squares; top and right axes). The former was measured at constant pH 9.1 and the latter at varying pHs. All other conditions as in Figure 4.

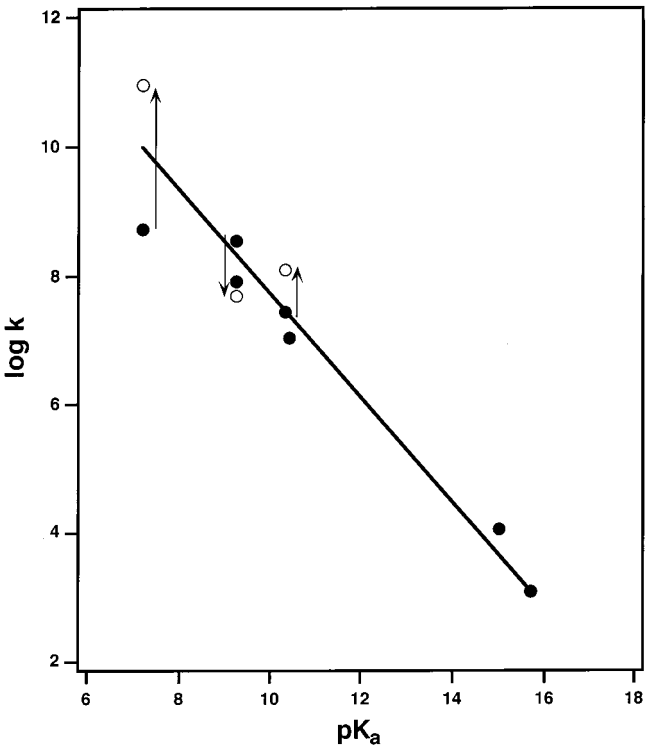


**Figure 6.** Free-energy correlation between the rate constant of protonation and the p$K_a$ of the corresponding general acid [points from left to right: $H_2PO_4^-$, $NH_4^+$, $B(OH)_3$, $CH_3OH$, $H_2O$]. Open circles and arrows indicate the correction of the rate constant for the electrostatic interactions between the reactants.

Figure 6 displays a free-energy correlation between the rate constant of the acids in Table 1 and their p$K_a$. The slope of the line in Figure 6 is 0.81. Correction of the rate constant for the electrostatic interaction between the radical dianion and charged acids (arrows in Figure 6) does not appreciably change the correlation. It can be noted that the reaction of boric acid is not strikingly outstanding in the correlation of Figure 6. Boric acid is outstandingly slow in similar free-energy correlations, when proton transfer is the rate-limiting reaction, even relative to acids of higher p$K_a$.[25] It is commonly accepted that boric acid acts as a general Lewis acid, a hydroxide ion acceptor as in eq 15.[26]

$$B(OH)_3 + H_2O \rightleftarrows B(OH)_4^- + H^+ \qquad (15)$$

The reaction of boric acid with $NO_3^{2-}$ is, therefore, better described as an $O^{2-}$ transfer analogous to reaction 14b.

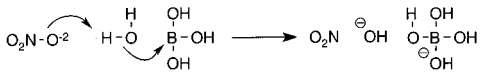


(14b)

It is easy to show that the sequence of reactions 2−8 is incompatible with the present observations and with earlier results. Assuming instantaneous equilibration of all the acid−base equilibria involved (reactions 3, 4, and 8), these equilibria are maintained during the decay of $NO_3^{2-}$. Then, the observed rate constant for its disappearance, at pHs where the doubly protonated form, $H_2NO_3$, is negligible, is given by eq 16.

$$k_{obs} = \frac{k_2 K_{a1} + k_5[H^+]}{K_{a1} + [H^+]} \qquad (16)$$

This represents the fastest disappearance of the dianion within the framework of the scheme discussed above, independent of the buffer and its concentration. At pH = p$K_{a1}$ = 7.5, eq 16 predicts the observed rate constant for $NO_3^{2-}$ disappearance should be $1.4 \times 10^5$ $M^{-1}$ $s^{-1}$, the average of the two decay rate constants, $k_2$ and $k_5$. However, the observed rate of $NO_3^{2-}$ decay in $5 \times 10^{-3}$ M phosphate buffer adjusted to pH 7.5 is more than an order of magnitude faster than predicted if equilibrium exists (reaction 7). As can be seen in Table 1, acids of p$K_a$ that are 3 units higher than the proposed p$K_a$ for $NO_3^{2-}$ still react fast with $NO_3^{2-}$.

The radiolytic reduction of nitrate to $NO_3^{2-}$ and the acid−base reactions that follow (reactions 1−6) are accompanied by significant conductivity changes that can conveniently be detected. Early experiments have already utilized this technique but conclusions regarding the identity of the products vary.[34,1] Barker et al. conclude from the small conductivity changes at the end of the protonation reaction that $HNO_3^-$ is not the product. We attempted to follow the protonation reactions of equilibria 3 and 4 using this technique but the results were inconclusive. At the near neutral pH required following reactions 3 and 4, the protonation is too slow to follow before the radical disappears. Furthermore, the conductivity signal inverts from increased to decreased conductivity due to the generation of protons by the pulse and their consumption by these reactions, thus complicating the analysis.

The kinetics indicates that the protonated intermediate is too short-lived to be detected. This conclusion concurs with a recent report of Mezyk and Bartels[27] who deduce, based on the activation parameters of reaction 17, that the hydrogen atom reaction with nitrate leads directly to the lose of hydroxide. Addition of H atom in reaction 17 would lead to the same

$$H + NO_3^- \rightarrow NO_2 + OH^- \qquad (17)$$

intermediate discussed above. Furthermore, the fast reaction of

**TABLE 2: Gas-Phase G2 and Solvation Energies of the $NO_3^-/NO_3^{2-}$ Couple and Their Monoprotonated Species**

| | | G2 energies (au) | | solvation energies (kcal/mol) | |
|---|---|---|---|---|---|
| species | symmetry | *E* (0 K) | *G* (298 K) | $\Delta H$ (0 K)[a] | $\Delta G$ (298 K)[b] |
| $NO_3^-$ | $D_{3h}$ | −280.04486 | −280.06858 | −83.0 | −63.8 |
| $NO_3^{-2}$ | $C_{3v}$ | −279.81330 | −279.83969 | −308.1 | −285.8 |
| $HNO_3$ | $C_1$ | −280.55876 | −280.58438 | | −3.8 |
| $HNO_3^-$(I)[c] | $C_1$ | −280.58184 | −280.60854 | −81.1 | −70.8 |
| $HNO_3^-$(II)[c] | $C_{2v}$ | −280.59115 | −280.62073 | | |
| $HNO_3^-$(III)[c] | $C_s$ | −280.59481 | −280.62398 | | |

[a] PCM model. [b] SM1 EF CS3 model. [c] I, II, and III refer to the corresponding structures in Figure 7.

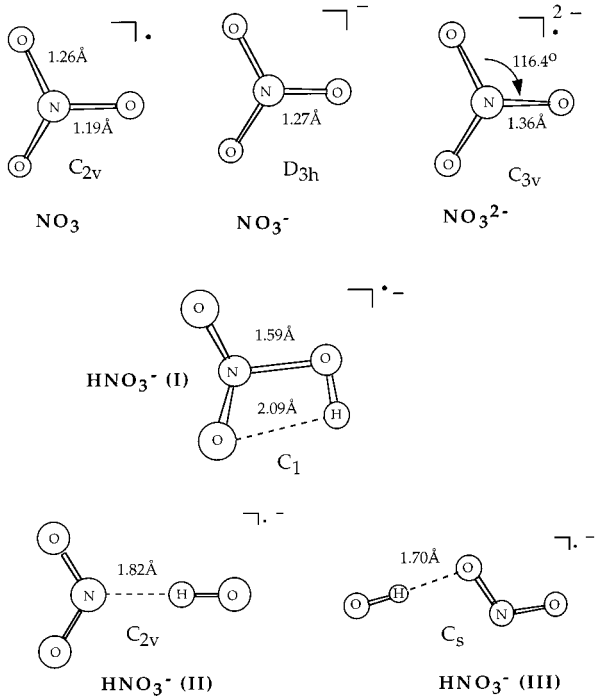


**Figure 7.** Optimized gas-phase structures of $NO_3^-$, $HNO_3^-$, and $NO_3^{2-}$ with selected MP2(full)/6-31G* geometry parameters.

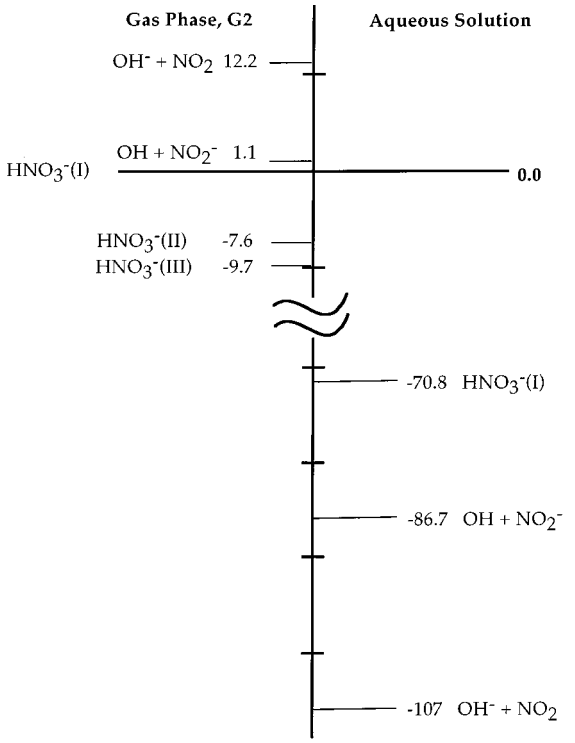


**Figure 8.** Relative energies (in kcal/mol) of $HNO_3^-$ and its dissociation products. Gas-phase energies are G2 free energies; For aqueous solution, solvation free energies were calculated using the SM1 model. I, II, and III refer to the corresponding structures in Figure 7.

the various acids with the radical dianion suggests that the reaction is not proton transfer. By inference to reaction 14a, $O^{2-}$ transfer to water seems to be the preferred route in the absence of added acids as well.

*Theoretical Estimates of Structure and Energies.* The G2 energies of the species relevant to the chemistry of $NO_3^{2-}$ are listed in Table 2. Because of the questions raised above regarding the observation of $HNO_3^-$, we focus in the calculations on this monoprotonated radical anion. The MP2(full)/6-31G* optimized gas-phase geometries used in the G2 calculations of $HNO_3^-$, $NO_3^-$, and $NO_3^{2-}$ with selected geometrical parameters are shown in Figure 7. Three local minima were identified for the structure of $HNO_3^-$ and all three correspond to loosely bound complexes between $NO_2^-$ and OH. No structures corresponding to complexes between $NO_2$ and $OH^-$ were found, probably because the electron affinity of $NO_2$ is significantly larger than that of OH (2.34 vs 1.87 eV respectively at the G2 level at 0 K, and 2.30 vs 1.83 eV experimentally determined).[28] Interestingly, the least stable (highest energy) structure, labeled I in Figure 7, is the structure most similar to $HNO_3$. This structure has an N−OH distance of 1.59 Å and N−O distances of 1.27 and 1.29 Å. Structures II and III are hydrogen-bonded complexes with OH−N and OH−O distances of 1.82 and 1.70 Å, respectively. The OH−O hydrogen-bonded complex is the most stable of the three and all are thermodynamically stable in the gas phase compared to the dissociated species, OH + $NO_2^-$ and $OH^-$ + $NO_2$.

The stability of $HNO_3^-$ and its products in aqueous solution were calculated using the PCM and SMx solvation models. The solvation energies and the relative stabilities in aqueous solution are summarized in Table 2 and Figure 8, respectively. It is expected that water complexes II and III are not important species as they are likely to dissociate and become individually solvated. Thus, only solvation of structure I was considered. The results in Figure 8 indicate that the dissociation products in aqueous solution are stabilized relative to $HNO_3^-$. The lowest energy products are $OH^-$ + $NO_2$, in contrast to the gas phase where the preferred products are OH + $NO_2^-$. It was indeed experimentally verified that electron attachment to $HNO_3$ leads in the gas phase to facile dissociation to OH + $NO_2^-$.[29] The present and many earlier results clearly show the change in products in aqueous solutions. The difference in aqueous solution results from the greater solvation energy of $OH^-$ relative to $NO_2^-$ (−109.8 vs −83.0 kcal/mol, respectively, Table 2). From the large stabilization energy, we expect only a small activation barrier. The gas-phase activation energy was calculated at the HF/6-31G* level to be ∼4.5 kcal $mol^{-1}$. This barrier is likely to be lower in solution.

**TABLE 3: Calculated Energies (in kcal mol$^{-1}$) for the $NO_3^{-2} \rightarrow NO_3^- + e^-$ Reaction from Different Methods**

| | method | $\Delta H$ (0 K)[a] | $\Delta G$ (298 K)[a] |
|---|---|---|---|
| | Gas-Phase G2 Energies (used for all cycle calculations) | | |
| $NO_3^{-2}(g) \rightarrow NO_3^-(g) + e^-(g)$ | G2 | −145.3 | −143.6 |
| | PCM Solvation Energies | | |
| $NO_3^{-2}(g) \rightarrow NO_3^{-2}(aq)$ | PCM[b] | −308.1 | |
| $NO_3^-(g) \rightarrow NO_3^-(aq)$ | PCM[b] | −83.0 | |
| $NO_3^{-2}(aq) \rightarrow NO_3^-(aq) + e^-(g)$ | PCM, G2 | 79.8 (−1.04) | |
| | SM1 Solvation Energies | | |
| $NO_3^{-2}(g) \rightarrow NO_3^{-2}(aq)$ | SM1 | | −285.8 |
| $NO_3^-(g) \rightarrow NO_3^-(aq)$ | SM1 | | −63.8 |
| $NO_3^{-2}(aq) \rightarrow NO_3^-(aq) + e^-(g)$ | SM1,G2 | | 78.4 (−1.10) |
| | SM2.2 Solvation Energies | | |
| $NO_3^{-2}(g) \rightarrow NO_3^{-2}(aq)$ | SM2.2 | | −282.1 |
| $NO_3^-(g) \rightarrow NO_3^-(aq)$ | SM2.2 | | −60.6 |
| $NO_3^{-2}(aq) \rightarrow NO_3^-(aq) + e^-(g)$ | SM2.2, G2 | | 77.9 (−1.12) |
| | DFT on $NO_3^{2-}\cdot 3H_2O$ Cluster | | |
| $NO_3^{-2}\cdot(H_2O)_3(g) \rightarrow NO_3^-\cdot(H_2O)_3(g) + e^-(g)$ | B3LYP[c] | −94.4 | |
| $NO_3^{-2}\cdot(H_2O)_3(g) \rightarrow NO_3^{-2}\cdot(H_2O)_3(aq)$ | PCM[b] | −239.2 | |
| $NO_3^-\cdot(H_2O)_3(g) \rightarrow NO_3^-\cdot(H_2O)_3(aq)$ | PCM[b] | −71.5 | |
| $NO_3^{-2}\cdot(H_2O)_3(aq) \rightarrow NO_3^-\cdot(H_2O)_3(aq)^{\bullet} + e^-(g)$ | PCM, B3LYP | 73.3 (−1.32) | |

[a] Values in parentheses are calculated redox potentials in eV vs NHE. The values derived from $\Delta H$ (0 K) do not include entropy terms. [b] From PCM calculation at the HF/6-31G* level. The nonelectrostatic part is neglected and should approximately cancel for this reaction. [c] From B3LYP Density Function Theory using 6-311+G(3df,2p) basis set at the HF/6-31G* energy optimized geometry.

**SCHEME 1: Thermodynamic Cycle To Calculate the Redox Free Energy of the $NO_3-/NO_3^{2}-$**

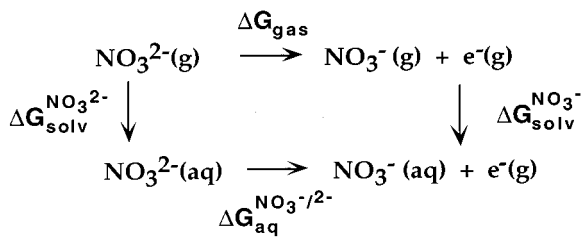


$$\Delta G_{aq}^{NO_3^{-/2-}} = \Delta G_{gas} + \Delta G_{solv}^{NO_3^-} - \Delta G_{solv}^{NO_3^{2-}}$$

The redox potential of the $NO_3^-/NO_3^{2-}$ couple was calculated using the thermodynamic cycle shown in Scheme 1.

The gas-phase enthalpy and free energy for the reaction $NO_3^{2-} \rightarrow NO_3^- + e^-$ were calculated using the G2 energies listed in Table 2. The normal hydrogen electrode (NHE) was taken as −4.5 V on the absolute scale. Results using several different calculation methods are summarized in Table 3. Not surprisingly, the dianion is unstable in the gas phase but it is stabilized by the very large solvation energy in aqueous solutions (in excess of 10 eV). The redox potential of the $NO_3^-/NO_3^{2-}$ couple is calculated to be −1.04 and −1.12 V vs NHE using the G2 reaction energies and either PCM or SMx solvation energies, respectively. The calculated redox potentials have uncertainties from both the G2 reaction energy and the solvation model. The uncertainty in the G2 method is ∼0.1 eV for most reaction energies, but it was not assessed for dianions. The solvation models have similar uncertainties. Thus, the uncertainty in the calculated values of the redox potential is approximately ±0.2 eV. These calculated redox potential served to guide our experimental effort in the selection of appropriate electron acceptors for pulse radiolytic estimation of the redox potential.

Since the accuracy of the G2 theory for dianions is not well established, we also carried out a calculation of the redox potential using an alternate solvation model in which three water molecules were explicitly placed around the anions. This calculation was done using density functional theory (DFT) with the B3LYP method[30] and the 6-311+G(3df,2p) basis set on fully optimized HF/6-31G* geometries. A calculation using the G2 method with this cluster would have been prohibitively lengthy. The PCM method was then used to obtain hydration energies of the complexes. The results for this calculation are also included in Table 3. A redox potential of −1.32 V vs NHE was obtained with this alternate method, approximately 0.25 V more negative than that obtained from the other methods.

*Redox Potential and Electron Transfer.* Barker estimated, from photocurrent experiments, that redox potential of the $NO_3^-/NO_3^{2-}$ couple is more negative than −0.86 V NHE.[31] Using pulse radiolysis we equilibrated the radical dianion with redox couples of known potentials (reaction 18). Because of the short lifetime of $NO_3^{2-}$, and because the rate of electron transfer

$$NO_3^{2-} + Q \rightleftarrows NO_3^- + Q^- \qquad (18)$$

slows significantly as the free energy of reaction 18 approaches zero, equilibrium 18 is difficult to achieve. Nonetheless, equilibrium was established in the case of the bipyridinium salt, $Q = V^{2+}$, described in the Experimental Section. All experiments on this issue were performed at pH 9.2 (1.0 mM Borax buffer), where $NO_3^{2-}$ is relatively long-lived. The products of reaction 18 were identified by their absorption spectra. They agree well with the reported spectra in the literature for $Q^-$ and with the spectra obtained upon direct reduction of Q by $e^-_{aq}$.

The equilibrium constant for reaction 18 was determined both from the yield of the $V^+$ radical and from the ratio of the rate constants $k_{18}/k_{-18}$ (measured at its absorption maxima of 520 and 385 nm) at various nitrate and $V^{2+}$ concentrations. As expected, the equilibrium constant is strongly dependent on ionic strength. Therefore, equilibrium and rate parameters were determined at constant $\mu = 0.2$. To obtain information at high concentrations (relevant to the high level radioactive waste), these parameter were also calculated for a wide range of concentrations. Equation 13, and essentially the same values, $Z_aZ_b = -4.0$ and $d = 2.45$ Å as obtained in Figure 2, were used to estimate the rate parameters at $\mu = 0$ from the results at $\mu = 0.2$. We obtain $k_{18}^{(o)} = 2.6 \times 10^{10}$ M$^{-1}$ s$^{-1}$, $k_{-18}^{(o)} = 2.3 \times$

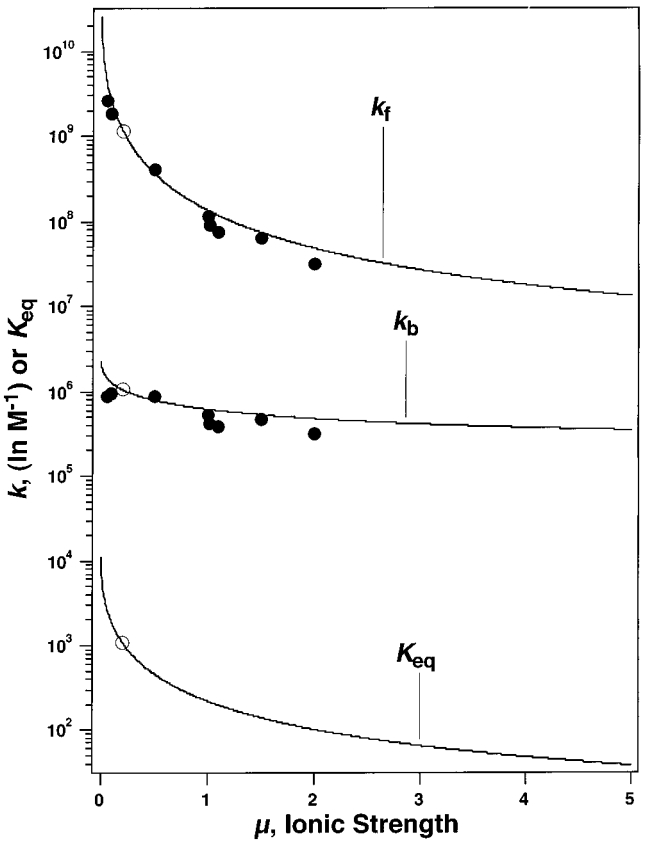


**Figure 9.** Ionic strength dependence of rate and equilibrium constants for electron transfer from $NO_3^{2-}$ to $V^{2+}$ and back (reaction 18). Circles are measured experimental results. Open circles are experimental results at $\mu = 0.2$, from which the individual parameters were taken for the calculation. At $\mu = 0$: $k_f = 2.6 \times 10^{10}$ M$^{-1}$, $k_b = 2.3 \times 10^6$ M$^{-1}$, $K_{eq} = 1.1 \times 10^4$.

$10^6$ M$^{-1}$ s$^{-1}$, and $K_{eq}^{(o)} = 1.1 \times 10^4$ using this procedure. The calculated dependence of the rate and equilibrium parameters on ionic strength are shown in Figure 9, together with experimental results collected at several other ionic strengths. As can be seen in Figure 9, the calculation based on the results at $\mu = 0.2$ yields rate constants which may be larger than the experimentally observed values in both directions by up to 50%. The theoretically calculated equilibrium constants are, however, within 20% of the observed values.

Using the equilibrium constants determined above one calculates a midpoint potential of $E_m = -0.89 \pm 0.02$ V for the $NO_3^-/NO_3^{2-}$ couple at pH 9.2 and $\mu = 0$. The error estimate allows a factor of 2 in the equilibrium constant. This value is close to the predicted estimates of the theoretical calculations ($-1.04$ V with $\sim$0.1 V error estimate). At a more commonly encountered ionic strength of $\mu = 1.0$, and at that same pH, we estimate $E_m = -0.79 \pm 0.02$ V.

Similar results within the experimental error, were obtained with *p*-nitrobenzonitrile [NBN; $E°_{NBN/NBN^-} = -0.60$ V measured by cyclic voltammetry at pH 7; p$K_{a(NBN^-)} = 2.55$][32,33] as a reference couple. However, the rate of the forward reaction of equilibrium 18 for Q = NBN is slower than that with $V^{2+}$, and therefore, simulation of the kinetics system were required in order to extract the rate and equilibrium parameters. The $NBN^-$ radical, which is stable (at least on the millisecond time scale) when generated directly upon reduction by $e^-_{aq}$, decays when generated via reaction 18 indicating that equilibrium is attained in this system also. On the other hand, $NO_3^{2-}$ does not reduce cobaltocene [up to 10 mM; $E°(Cp_2Co^+/Cp_2Co) = -1.09$ V] during its lifetime.

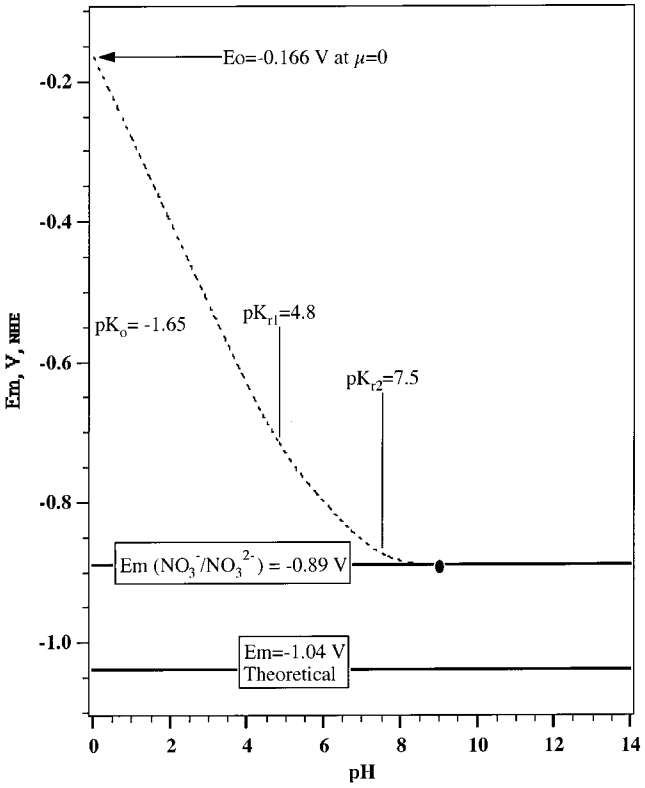


**Figure 10.** Redox potentials of the $NO_3^-/NO_3^{2-}$ couple. Dotted line is the calculated pH dependence of $E_m$ assuming the indicated, presently accepted, p$K_a$'s, that we question in this work. Solid point is the experimentally determined value; solid lines indicate the independence of the redox potential of pH.

The value for the formal redox potential of the $NO_3^-/NO_3^{2-}$ couple is coupled to its p$K_a$ values. If reversible acid−base equilibria can be obtained and the p$K_a$ values reported in the literature are used, then the formal potential (at 1 M $H^+$) is $E° = -0.16$ V. As discussed earlier, however, we believe that the protonated radical species are too short-lived to observe and their p$K_a$ values are questionable. Accordingly, the formal redox potential is pH independent. These two extreme views of the pH dependence of the couple, which reflect the stability of the protonated radical, are shown in Figure 10. The implications of this value of the redox potential and its pH dependence have been recently discussed.[38]

Of particular interest in the context of the chemistry in high level nuclear waste is the possible reaction of $NO_3^{2-}$ with nitrite. Because of the high concentration of nitrite in these systems, even a relatively small rate constant may imply an efficient conversion of $NO_3^{2-}$ to $NO_2^{2-}$ and eventually to NO. We, therefore, attempted to measure the rate constant of reaction 19.

$$NO_3^{2-} + NO_2^- \rightarrow NO_3^- + NO_2^{2-} \qquad (19)$$

Competition experiments between the bipyridinium ion $V^{2+}$ (at 1 mM) and nitrite (up to 1 M) for $NO_3^{2-}$ were performed at 1-M nitrate. It was verified that the product of reaction 19, the $NO_2^{2-}$ radical, does not generate $V^+$ in experiments where nitrite is reduced by $e^-_{aq}$. No significant reduction in the yield of $V^+$ (beyond that expected from Figure 2) was observed. We estimate an upper limit for the rate constant $k_{19} \leq 5 \times 10^4$ M$^{-1}$ s$^{-1}$. Whereas this is a relatively slow rate constant, we cannot rule out the possibility that the reduction equivalents are partially converted to NO via reaction 19 in highly concentrated nitrite

solutions. Furthermore, we will show in a separate report that reaction 19 is thermodynamically favorable.[39]

Another question of interest in the same context is the possible reduction of the nitrate ion by organic reducing radicals, R•. Attempts to measure the rate constant for reaction 20 for several reducing radicals failed indicating that the rate is too slow to measure. An upper limit

$$R^{\bullet} + NO_3^- \rightarrow R^+ + NO_3^{2-} \qquad (20)$$

for the rate constant of one of the strongest reducing radicals, $CO_2^-$ ($E_0 = -1.90$ V), was estimated from a competition between nitrate and cobaltocene for $CO_2^-$. No reduction in the yield of $(Cp_2)Co$ could be observed in solutions containing up to 0.1 M $NaNO_3$ and 0.2 M formate ions at pH 9, leading to an estimate of $k_{20} \leq 10^6$ $M^{-1}$ $s^{-1}$. The only report of one-electron reduction of nitrate, by any radical other than $e^-_{aq}$, indicates extremely low reduction rates. A value of $k_{20} = 28$ $M^{-1}$ $s^{-1}$ for $R^{\bullet} = (CH_3)_2COH$ was estimated from the yield of $NO_3^-$ destruction in steady-state radiolysis of nitrate solutions containing 2-propanol and acetone.[36]

## Conclusions

Because of the significance of radiolysis of nitrate/nitrite solutions in practical systems, especially in high-level nuclear waste, we revisited the reduction processes that follow irradiation of nitrate solutions. We find that the dianion obtained upon reaction of $e^-_{aq}$ with nitrate, $NO_3^{2-}$, is a strong reductant. We determined the redox potential of the $NO_3^-/NO_3^{2-}$ couple and its ionic strength dependence. The radical obtained upon reduction by the precursor to the solvated electron is similar to that obtained from $e^-_{aq}$, and the yield of the dianion radical is essentially unchanged even at very high nitrate concentrations. We also determined the rate constants of several general acids with the dianion and we suggest that the reaction is a dissociative $O^{2-}$ (i.e., water or hydroxide ions) transfer to the acid to yield directly the $NO_2$ radical. Therefore, the redox potential of that couple is pH independent. We discuss the implications of these observations to practical scenarios and we propose that the electron-transfer reaction from $NO_3^{2-}$ to nitrite, at high $NO_2^-$ concentration, may divert the chemistry from $NO_2$-based to NO-based chemistry in nuclear applications.

**Acknowledgment.** Support by the U.S. Department of Energy (DOE), Office of Basic Energy Sciences, Division of Chemical Sciences, and the Environmental Management Science Program is gratefully acknowledged. Argonne National Laboratory is operated by the University of Chicago under Contract W-31-109-ENG-38 with the DOE. This is document NDRL 4148 from the Notre Dame Radiation Laboratory.

## References and Notes

(1) Gratzel, M.; Henglein, A.; Taniguchi, S.; *Ber. Bunsen-Ges. Phys. Chem.* **1970**, *74*, 292.
(2) Buxton, G. V.; Greenstock, C. L.; Helman, W. P.; Ross, A. B. *J. Phys. Chem. Ref. Data* **1988**, *17*, 513.
(3) Stanbury, D. M. In *Advances in Inorganic Chemistry*; Sykes, A. G., Ed.; Academic Press: San Diego, 1989; p 69.
(4) Logager, T.; Sehested, K. *J. Phys. Chem.* **1993**, *97*, 10047.
(5) Benderskii, V. A.; Krivenko, A. G.; Ponomarev, E. A.; Federovich, N. V. *Sov. Electrochem.* **1987**, *23*, 1343.
(6) Homer, R. F.; Tomlinson, T. E. *J. Chem. Soc.* **1960**, 2498.
(7) Amouyal, E.; Zidler, B.; Keller, P.; Moradpour, A. *Chem. Phys. Lett.* **1980**, *74*, 314.
(8) Schmidt, K. H.; Han, P.; Bartels, D. M. *J. Phys. Chem.* **1995**, *99*, 10530.
(9) Hehre, W. J.; Radom, L.; Schleyer, P. v. R.; Pope, J. A. *ab initio Molecular Orbital Theory*; John Wiley & Sons: New York, 1986; 548.
(10) Curtiss, L. A.; Raghavachari, K.; Redfern, P. C.; Pople, J. A. *J. Chem. Phys.* **1997**, *106*, 1063.
(11) Curtiss, L. A.; Raghavachari, K.; Trucks, G. W.; Pople, J. A. *J. Chem. Phys.* **1991**, *94*, 7221.
(12) Frisch, M. J., et al. *Gaussian 94*, D.1 ed.; Gaussian Inc.: Pittsburgh, PA., 1995.
(13) Miertus, S.; Tomasi, J. *Chem. Phys.* **1982**, *65*, 239.
(14) Hawkins, G. D.; Lynch, G. C.; Giesen, D. J.; Rossi, I.; Storer, J. W.; Liotard, D. A.; Cramer, C. J.; Truhlar, D. G. *AMSOL*, 5.4 ed.; Hawkins, G. D., Lynch, G. C., Giesen, D. J., Rossi, I., Storer, J. W., Liotard, D. A., Cramer, C. J., Truhlar, D. G., Eds.; program 606 of the Quantum Chemistry Program Exchange: Indiana University, Bloomington IN.
(15) Cramer, C. J.; Truhlar, D. G. *J. Am. Chem. Soc.* **1991**, *113*, 8305.
(16) Gratzel, M.; Henglein, A.; Lilie, J.; Beck, G. *Ber. Bunsen-Ges. Phys. Chem.* **1969**, *73*, 646.
(17) Forni, L. G.; Mora-Arellano, V. O.; Packer, J. E.; Willson, R. L. *J. Chem. Soc., Perkin Trans.* **1986**, *2*, 1.
(18) Wolff, R. K.; Bronskill, M. J.; Hunt, J. W. *J. Chem. Phys.* **1970**, *53*, 4211.
(19) Lam, K. Y.; Hunt, J. W. *Int. J. Radiat. Phys. Chem.* **1975**, *7*, 317.
(20) Daniels, M. *J. Phys. Chem.* **1966**, *70*, 3022.
(21) Daniels, M. *Adv. Chem. Ser.* **1968**, *81*, 153.
(22) Daniels, M. *J. Phys. Chem.* **1969**, *73*, 3710.
(23) Daniels, M.; Wigg, E. E. *J. Phys. Chem.* **1969**, *73*, 3703.
(24) Kiwi, J. T.; Daniels, M. *J. Inorg. Nucl. Chem.* **1978**, *40*, 576.
(25) Kankaanpera, A.; Salomaa, P. *Acta Chem. Scand.* **1969**, *23*, 712.
(26) Greenwood, N. N. *Comprehensive Inorg. Chem.*; Greenwood, N. N., Ed.; 1973; Vol. 1, p 886.
(27) Mezyk, S. P.; Bartels, D. M. *J. Phys. Chem. A* 1997; *101*, 6233.
(28) Lias, S. G.; Bartmess, J. E.; Liebman, J. F.; Holmes, J. L.; Levin, R. D.; Mallard, W. G. *J. Phys. Chem. Ref. Data* **1988**, *17* (Suppl.), 861.
(29) Fehsenfeld, F. C.; Howard, C. J.; Schmeltekopf, A. L. *J. Chem. Phys.* **1975**, *63*, 2835.
(30) Becke, A. D. *J. Chem. Phys.* **1993**, *98*, 5648.
(31) Barker, G. C. *Ber. Bunsen-Ges. Phys. Chem.* **1971**, *75*, 728.
(32) Grunbein, W.; Fojtik, A.; Henglein, A.; Naturforsch, Z. **1969**, *24*, 1336.
(33) Rajh, T.; Vucemilovic, M. I.; Dimitrijevic, N. M.; Micic, O. I.; Nozik, A. J. *Chem. Phys. Lett.* **1988**, *143*, 305.
(34) Barker, G. C.; Fowles, P.; Stringer, B. *Trans. Faraday Soc.* **1970**, *66*, 1509.
(35) Gonzalez, M. C.; Braun, A. M. *Res. Chem. Intermed.* **1995**, *21*, 837.
(36) Henglein, A. *Ber. Bunsen-Ges. Phys. Chem.* **1980**, *84*, 253.
(37) Alfassi, Z. B.; Dhanasekaran, T.; Huie, R. E.; Neta, P. *Rad. Phys. Chem.* **1999**, *56*, 475.
(38) Fessenden, R. W.; Meisel, D.; Camaioni, D. M. *J. Am. Chem. Soc.* **2000**, *122*, 3773.
(39) Dimitrijevic, N.; Cook, A. R.; Curtiss, L. A.; Meisel, D.; Camaioni, D. Manuscript in preparation.
(40) See Cotton, F. A.; Wilkinson, G. *Advanced Inorganic Chemistry*, 5th ed.; John Wiley & Sons: New York; 1988; pp 105−107. We thank a reviewer for pointing this out to us.